research article

Multimodality CT imaging contributes to improving the diagnostic accuracy of solitary pulmonary nodules: a multi-institutional and prospective study

Gaowu Yan[1], Hongwei Li[2], Xiaoping Fan[1], Jiantao Deng[1], Jing Yan[1], Fei Qiao[3], Gaowen Yan[4], Tao Liu[1], Jiankang Chen[1], Lei Wang[1], Yang Yang[1], Yong Li[1], Linwei Zhao[1], Anup Bhetuwal[5], Morgan A McClure[6], Na Li[7], Chen Peng[8]

[1] Department of Radiology, Suining Central Hospital, Suining, China
[2] Department of Radiology, The Third Hospital of Mianyang and Sichuan Mental Health Center, Mianyang, China
[3] Department of CT and MRI, The First Affiliated Hospital, Shihezi University School of Medicine, Shihezi, China
[4] Department of Radiology, The First People's Hospital of Suining, Suining, China
[5] Sichuan Key Laboratory of Medical Imaging and Department of Radiology, Affiliated Hospital of North Sichuan Medical College, Nanchong, China
[6] Department of Radiology and Imaging; Institute of Rehabilitation and Development of Brain Function, The Second Clinical Medical College of North Sichuan Medical College Nanchong Central Hospital, Nanchong, China
[7] Department of Oncology, Suining Central Hospital, Suining, China
[8] Department of Gastroenterology, The First People's Hospital of Suining, Suining, China

Radiol Oncol 2023; 57(1): 20-34.

Received 15 August 2022
Accepted 5 December 2022

Correspondence to: Yong Li, Department of Radiology, Suining Central Hospital, Suining, China. E-mail: 13890893057@163.com and Na Li, Department of Oncology, Suining Central Hospital, Suining, China. E-mail: lny2008hy@163.com and Gaowu Yan, Department of Radiology, Suining Central Hospital, Suining, China. E-mail: yangaowu1989@163.com

Gaowu Yan, Hongwei Li, Xiaoping Fan, Jiantao Deng, Jing Yan, and Fei Qiao all have contributed equally to this study.

Disclosure: No potential conflicts of interest were disclosed.

Background. Solitary pulmonary nodules (SPNs) are one of the most common chest computed tomography (CT) abnormalities clinically. We aimed to investigate the value of non-contrast enhanced CT (NECT), contrast enhanced CT (CECT), CT perfusion imaging (CTPI), and dual- energy CT (DECT) used for differentiating benign and malignant SPNs with a multi-institutional and prospective study.

Patients and methods. Patients with 285 SPNs were scanned with NECT, CECT, CTPI and DECT. Differences between the benign and malignant SPNs on NECT, CECT, CTPI, and DECT used separately (NECT combined with CECT, DECT, and CTPI were methods of A, B, and C) or in combination (Method A + B, A + C, B + C, and A + B + C) were compared by receiver operating characteristic curve analysis.

Results. Multimodality CT imaging showed higher performances (sensitivities of 92.81% to 97.60%, specificities of 74.58% to 88.14%, and accuracies of 86.32% to 93.68%) than those of single modality CT imaging (sensitivities of 83.23% to 85.63%, specificities of 63.56% to 67.80%, and accuracies of 75.09% to 78.25%, all $p < 0.05$).

Conclusions. SPNs evaluated with multimodality CT imaging contributes to improving the diagnostic accuracy of benign and malignant SPNs. NECT helps to locate and evaluate the morphological characteristics of SPNs. CECT helps to evaluate the vascularity of SPNs. CTPI using parameter of permeability surface and DECT using parameter of normalized iodine concentration at the venous phase both are helpful for improving the diagnostic performance.

Key words: solitary pulmonary nodule; non-enhanced computed tomography; contrast-enhanced computed tomography; computed tomography perfusion imaging; dual-energy computed tomography

Introduction

A solitary pulmonary nodule (SPN) is defined as a focal, round or oval area of increased opacity in the lung with its maximum diameter no larger than 3.0 cm.[1-3] It is also one of the most common chest radiography (CR) or computed tomography (CT) abnormalities that are often identified incidentally in clinical practice with 150,000 SPNs incidentally detected in the United States on CR or CT every year.[1] It is estimated that the prevalence of SPNs in the general population is about 2.0% to 24.0%. Among those with more risk factors of lung malignancies (*e.g.* an older age, male, history of smoking or tumor, *etc.*), the prevalence of a SPN is up to 17.0% to 53.0%.[4] With the generally increased use of CT worldwide, it can be understood that more SPNs will be detected in the coming years.

The etiology of SPNs includes neoplasms (*e.g.*, primary pulmonary carcinoma, solitary metastasis, or chondroma), infection (*e.g.*, infectious granuloma or round pneumonia), inflammation (*e.g.*, rheumatoid arthritis or granulomatosis with polyangiitis), vascular (*e.g.*, arteriovenous malformation, infarct, or hematoma) and congenital abnormities (*e.g.*, sequestration or bronchogenic cyst). As a result, it is important to accurately distinguish between benign and malignant SPNs before invasive managements; especially for solid nodules with sizes of ≥ 15 mm (≥ 1767 mm^3). As the Lung-RADS guidelines have reported that their risk of malignancy is more than 15%.[2] This is because for benign SPNs, conservative treatments such as drugs or observation may suffice. While for lung cancer and other malignant SPNs, we usually need surgical treatments as soon as possible.

Compared with CR, magnetic resonance imaging (MRI), and positron emission tomography (PET), a CT plays an important role in the diagnosis and management of SPNs.[1-3,5,6] For conventional CT (non-contrast enhanced CT, NECT), it is usually used to evaluate the size, margins, contour, and internal characteristics of a SPN. For contrast enhanced CT (CECT), it helps evaluate the vascularity of a SPN. With the development of CT technologies, CT perfusion imaging (CTPI) and dual-energy CT (DECT) are increasingly used in clinical practice.[7-10] For example, in a study by Wen *et al.*[10], quantitative measures (the slope of the spectral Hounsfield Unit (HU) curve (λ_{HU}), normalized iodine concentration (NIC), CT values of 40 keV monochromatic images (CT_{40keV}), and normalized arterial enhancement fraction (NAEF)) from DECT can help to differentiate benign from malignant SPNs.

We hypothesized that multimodality CT imaging may contribute to improving the diagnostic accuracy of SPNs. However, to the authors' knowledge, there are no publications in the literature in which NECT, CECT, CTPI and DECT were comprehensively used to differentiate benign or malignant SPNs. Thus, the aim of this study was to investigate the value of NECT, CECT, CTPI, and DECT in the differentiation of benign or malignant SPNs with a multi-institutional and prospective study.

Patients and methods

Patients

This study was conducted at our three teaching hospitals and approved by the institutional review committee of Suining Central Hospital (Suining, China; approval no. LLSNCH20200004). All patients were included after providing informed consent.

Patients with SPNs were admitted and treated at one of the three hospitals from January 2019 to June 2021 and were consecutively enrolled into our study. The inclusion criteria were: (1) SPNs were detected with NECT in the lung window; (2) each SPN size is 1.5 cm–3.0 cm; (3) benign or malignant SPNs were confirmed by CT-guided percutaneous biopsy or pathology after surgery; (4) CTPI and DECT were performed within one week prior to CT-guided percutaneous biopsy or surgery; (5) SPNs were not treated by any antitumor therapies (*e.g.*, radiotherapy, chemotherapy, or targeted drug therapy); (6) age > 18 years old; and (7) patients had acceptable liver and kidney functions and no history of allergies (for example, allergic to iodine or seafood). The exclusion criteria were: (1) SPNs appearing as pure ground-glass opacity (pGGO) or as subsolid nodules that could not be measured in the mediastinal window; (2) majority components of the SPNs have been calcified or liquefactive necrosis, leading to region of interests (ROIs) cannot be drawn; (3) body mass index (BMI) is greater than 30.0 kg/m^2; (4) poor image quality (*e.g.*, significant anomalies by heart beats or others artifacts); and (5) incomplete clinical data. Three hundred and twenty-three patients were included and 38 of them were excluded because of the exclusion criteria (Figure 1).

CT examination

All patients were scanned with the same DECT system (Revolution CT, GE Healthcare, Milwaukee,

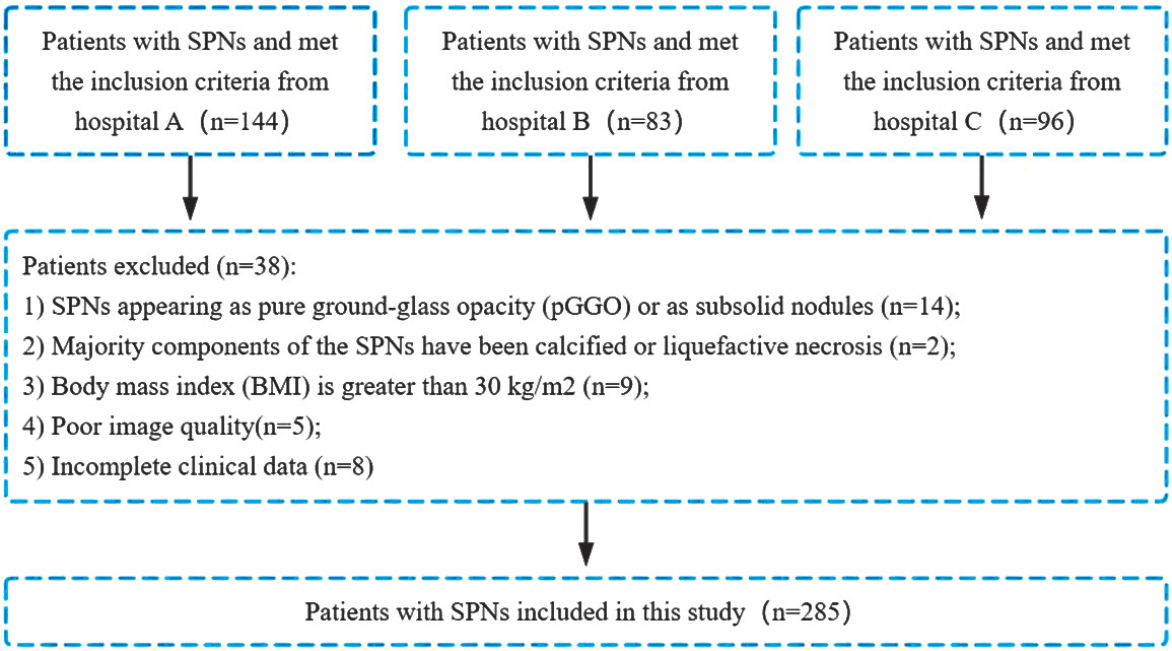

FIGURE 1. Flow chart of patient selection.

SPNs = solitary pulmonary nodules

WI, USA), and all the scanning parameters were set at the same level. The multimodality CT imaging protocol included three steps, *i.e.*, NECT, CTPI, and DECT.

For NECT, the patients were asked to hold their breath at the end of inspiration, and the scanning ranges were taken from the thoracic inlet to the bilateral costophrenic angle. The tube voltage was 100 kVp; the tube current was modulated by a SmartmA technology, which provides reasonable tube current to decrease the radiation dose; and the preset noise index was adjusted for patient circumference.

For CTPI, the patients were asked to take relaxed and slow respiration. After the position of an SPN was determined by the NECT, a GSI Chest Perfusion protocol was used with a scanning range of 3.0 cm above and below the central level of a SPN. A non-ionic iodine contrast agent of 400 mg/ml (Iomeron®, Shanghai Braccosine Pharmaceutical Co., Ltd.) was injected into an antecubital vein with a binocular power injector (Stellant D-CE, MEDRAD, Bayer Healthcare Co., Ltd.), at a flow rate of 5.0 ml/s (40.0 ml). After that, 20.0 ml of normal saline at a speed of 5.0 ml/s was used to flush the tube. The CTPI was performed after injection of the contrast medium with a delay time of 4.0 s. The tube voltage and tube current were 70 kVp and 250 mA respectively. There were 18 scanning phases with an interval of 2.5 s, and the total acquisition time was about 43.0 s.

For DECT, the patients were asked to hold their breath at the end of inspiration, and the scanning ranges were the same as the NECT. Another 50.0 ml contrast agent was injected into the antecubital vein with the binocular power injector, at a flow rate of 2.5 ml/s. After that, 20.0 ml of normal saline at a speed of 2.5 ml/s was used to flush the tube. A ROI was placed in the thoracic aorta at the level of bronchial bifurcation, and the threshold was set to 120 HU. After reaching the threshold, the arterial phase was scanned with a delay time of 7.0 s, and the venous phase delay time was 30.0 s. The tube voltage, tube current, and noise index were the same as the NECT.

The same scanning parameters for NECT, CTPI, and DECT were: detector coverage = 80 mm; pitch = 0.992: 1; coverage speed = 158.75 mm/s; rotation time = 0.5 s; preset adaptive statistical iterative reconstruction-V (ASIR-V) = 50%; postset ASIR-V = 60%; slice thickness = 5.0 mm; slice interval = 5.0 mm; reconstructed slice thickness = 1.25 mm; reconstructed slice interval = 1.25 mm.

Measurement of radiation dose

After the multimodality CT imaging protocol, the volume CT dose index ($CTDI_{vol}$, mGy) and dose-

length product (DLP, mGy.cm) were recorded. The estimated effective dose (ED, mSv) was calculated with the formula: ED = DLP × *k*, where the *k* equals 0.014 mSv/mGy.cm.

Images post-processing

For NECT, the lung window images were further processed with the post-processing workstation AW 4.7 (GE Healthcare, Milwaukee, WI, USA) to obtain multiplanar reconstruction (MPR) coronal and sagittal images (1.25 mm).

For CTPI, the images were transferred to the post-processing workstation AW 4.7 (GE Healthcare, Milwaukee, WI, USA), CTPI parameters of the blood volume (BV, ml/100 g), blood flow (BF, ml/100 g/min), mean transit time (MTT, s), and permeability surface (PS, ml/100 g/min) with their perfusion artificial color maps were automatically generated by the CT perfusion 4D software. The ROI should be placed in the soft tissue area of a SPN at its maximum plane, and the thoracic aorta at the same level plane was selected as the reference vessel for calculating the arterial input function and a time density curve (TDC). When placing a ROI, the calcification, bleeding, liquefaction necrosis area, blood vessels, and anomalies by heart beats or other artifacts should be avoided as much as possible.

For DECT, the arterial and venous phase mediastinal window images were respectively processed with the GSI volume viewer software (AW 4.7, GE Healthcare, Milwaukee, WI, USA), to obtain the arterial and venous phase iodine-based images. The following principles should be followed in outlining the ROI: (1) ROI should be placed in the solid area of a SPN with uniform enhancement, and the outlined area should be as large as possible; (2) the calcification, bleeding, liquefaction necrosis area, blood vessels, and anomalies by heart beats or others artifacts should be avoided as much as possible; (3) the position and size of ROI measurement in each phase should be consistent.

Parameter measurements

The parameter measurements for CTPI, DECT, and the CT enhancement amplitude value were independently measured by two senior radiologists with more than 15 years of experience in chest CT. All indices were measured two times, and the average values were taken as the final results. Disagreements were resolved through consensus. Parameter measurements for CTPI included BV, BF, MTT, and PS. Parameter measurements for DECT included iodine overlay (OL), iodine concentration (IC), and normalized iodine concentration (NIC) at the arterial and venous phases (*i.e.*, aOL, vOL, aIC, vIC, aNIC, and vNIC). The NIC was calculated with the formulae: $NIC = IC_{SPN} / IC_{Thoracic\ aorta}$. The CT values of a SPN at the venous CECT and NECT phases were also measured, and the CT enhancement amplitude value was calculated with the formula: CT enhancement amplitude value = venous CECT value - NECT value.

Multimodality CT imaging for evaluating SPN

First, another two senior radiologists with more than 15 years of experience in chest CT randomly and independently interpreted the conventional NECT images of each SPN. Any disagreements were solved through consensus. The SPNs were then classified into five categories, *i.e.*, I = most likely benign, II = possibly benign, III = uncertain benign or malignant, IV = possibly malignant, and V = most likely malignant. The diagnostic methods were as follows: NECT combined with CECT (Method A), and the diagnostic criteria for CT enhancement were[1]: a CT enhancement amplitude value of 20–60 HU was classified as malignant, and a CT enhancement amplitude value of less than 20 HU or more than 60 HU was classified as benign; NECT combined with DECT (Method B); NECT combined with CTPI (Method C). If methods A, B, or C were consistent when classifying a benign or malignant SPN, the SPN would be judged as benign or malignant. However, if methods A, B, or C were not consistent when classifying a benign or malignant SPN, the following principles would be followed: (1) if a benign or malignant SPN was definitely diagnosed as category I or V by NECT, the diagnostic results of CECT, DECT and CTPI would not be considered, and the SPN would be directly characterized as benign or malignant; (2) if the nature of a benign or malignant SPN could not be confirmed by NECT (*i.e.* a category of II, III or IV SPN), the final diagnosis would be made according to the diagnostic thresholds of CECT, DECT and CTPI, respectively. There were four combined diagnostic methods: method A + B, method A + C, method B + C, and method A + B + C (Figure 2). In combined diagnostic methods, the results of benign or malignant SPNs may be inconsistent according to the diagnostic thresholds of CECT, CTPI or DECT. Our method is that if a SPN is diagnosed as malignant according to one of

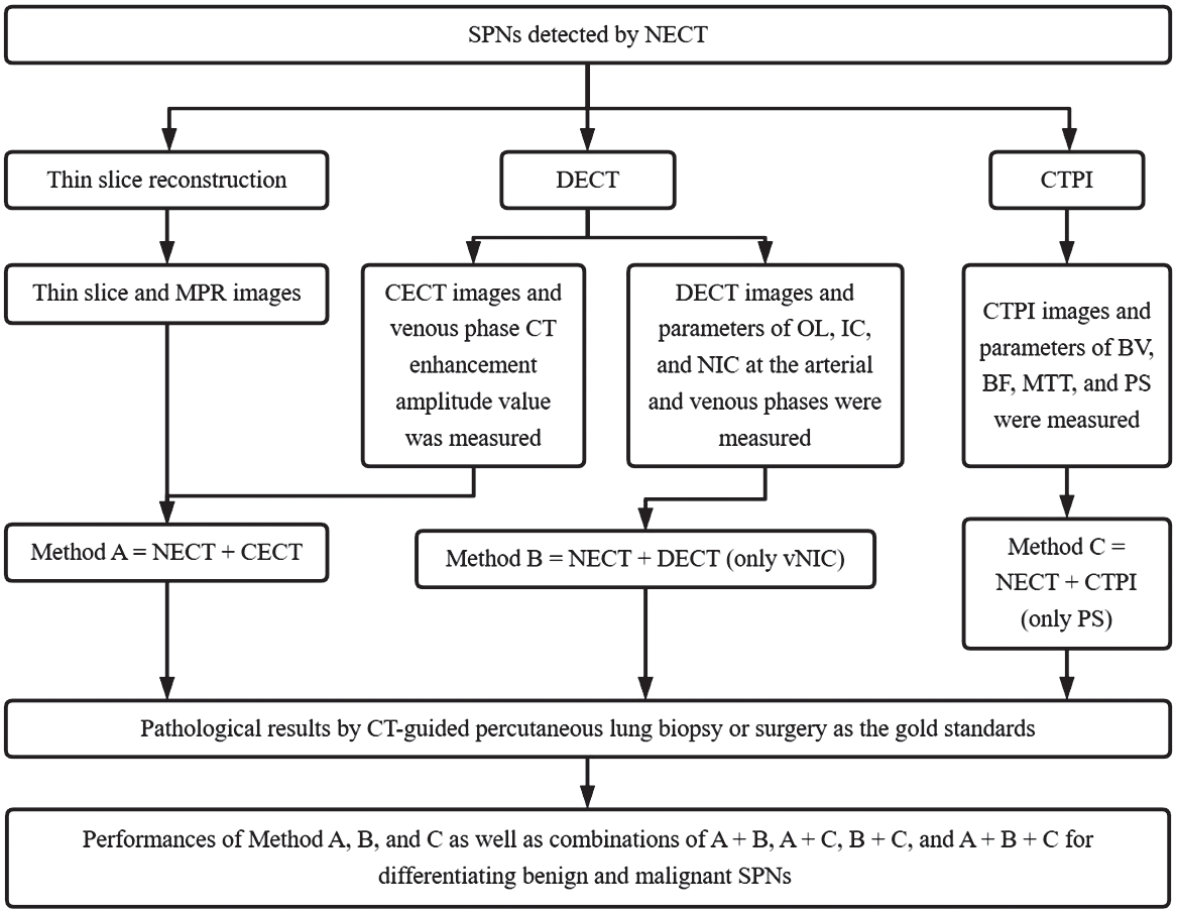

FIGURE 2. Technology roadmap of multimodality computed tomography (CT) imaging for evaluating solitary pulmonary nodules (SPNs).

BF = blood flow; BV = blood volume; CECT = contrast enhanced CT; CTPI = CT perfusion imaging; DECT = dual-energy CT; IC = iodine concentration; MPR = multiplanar reconstruction; NECT = non-contrast enhanced CT; MTT = mean transit time; NIC = normalized iodine concentration; OL = iodine overlay; PS = permeability surface

the thresholds (CECT, CTPI, or DECT), it would be preliminarily categorized as malignant; then, the result would be compared with the pathological result to calculate the sensitivity, specificity and accuracy of the combined diagnostic method.

Statistical analysis

Measurement data were expressed as the mean ± standard deviation or median and interquartile range (P_{25}, P_{75}). The comparisons were performed with the two independent samples *t*-test or Mann Whitney rank sum test, as appropriate. The count data were expressed as the percentage (%) or composition, and the comparisons were performed with the Fisher's exact test. Receiver operating characteristic (ROC) curve analysis was performed on statistically significant CTPI and DECT parameters to obtain the area under the curves (AUC) and diagnostic thresholds, and the Delong-test was performed to compare the differences.[11]

In using the pathological diagnosis as the gold standard, the sensitivities, specificities, accuracies, positive predictive values (PPVs) and negative predictive values (NPVs) of the three diagnostic methods separately used (Method A, B, and C) and in combination (Method A + B, Method A + C, Method B + C, and Method A + B + C) for the diagnosis of benign and malignant SPNs were calculated, and the McNemar's test was used to compare the sensitivity, specificity, and accuracy of the various diagnostic methods.

All statistical analyses were performed by using the software of GraphPad Prism 8.0.0 and MedCalc 19.5.3. Significant differences were set at a p value < 0.05.

Results

Patient characteristics

Ultimately, 285 SPNs were included in this study. Of these, 178 (62.46%, 178/285) SPNs were confirmed by CT-guided percutaneous biopsy, and 107 (37.54%, 107/285) SPNs were confirmed by pathology after surgery. The patients' characteristics are shown in Table 1. There were no significant differences between the malignant and benign SPNs relative to gender, age, smoking status, history of tumors, or tumor biomarkers (all p values > 0.05).

Pathological results

Of the 285 SPNs, 118 were benign SPNs (41.4%, 118/285) and 167 were malignant SPNs (58.6%, 167/285). Of the 118 benign SPNs, 46 were tuberculosis (29.0%, 46/118), 32 were acute and chronic inflammation (27.1%, 32/118), and 14 were inflammatory pseudotumors (11.9%, 14/118). Of the 167 malignant SPNs, 116 (69.5%, 116/167) were primary pulmonary carcinomas (including adenocarcinomas in 52, squamous cell carcinomas in 35, and small cell lung cancer in 17, *etc*.), 23 (13.8%, 23/167) were solitary metastasis (this included five from the liver, five from the breast, etc). Pathological results of the 285 SPNs included in this study are shown in Table 2.

Radiation dose

After the multimodality CT imaging protocol, the $CTDI_{vol}$, DLP, and ED in the SPNs were 66.88 ± 4.36 mGy, 768.29 ± 91.65 mGy.cm, and 10.76 ± 1.28 mSv, respectively.

NECT and CECT in evaluating SPNs

In the malignant SPNs (n = 167), 49 (29.34%, 49/167), 115 (68.86%, 115/167), 108 (78.81%, 108/167), 38 (22.75%, 38/167), 89 (53.29%, 89/167), and 84 (50.30%, 84/167) cases were seen with smooth margins, lobulated sign, spiculated sign, vacuole sign, pleural indentation, and vessel convergence, respectively. In the benign SPNs (n = 118), the same CT findings were seen in 84 (71.19%, 84/118), 29 (24.58%, 29/167), 25 (21.19%, 25/118), 13 (11.02%, 13/118), 25 (21.19%, 25/118), and 33 (27.97%, 33/118) cases (Table 3), respectively. There were significant differences between the malignant and benign SPNs in above mentioned findings on NECT (all p values were < 0.05). However, no significant differences were noted between the malignant and benign SPNs in cavity sign, air bronchogram, calcification, fat (defined as CT attenuation of -40 HU to -120 HU), adjacent bronchial changes, location, or size on NECT (all p values were > 0.05).

TABLE 1. Patient characteristics in 285 patients with solitary pulmonary nodules

Characteristics	Pathology		*P* value
	Benign SPNs (n = 118)	Malignant SPNs (n = 167)	
Gender*			
Male	56 (47.46%)	96 (57.49%)	0.1170
Female	62 (52.54%)	71 (42.51%)	
Age (years)#	50.84 ± 19.60	52.93 ± 20.30	0.3952
Smoking status*			
Yes	52 (44.07%)	81 (48.50%)	0.4721
No	66 (55.93%)	86 (51.50%)	
Tumor history*			
Yes	17 (14.41%)	28 (16.77%)	0.6245
No	101 (85.59%)	139 (83.23%)	
Tumor biomarkers*			
Normal	103 (87.29%)	139 (83.23%)	0.4026
Abnormal	15 (12.71%)	28 (16.77%)	

SPNs = solitary pulmonary nodules; *compared with the Fisher's exact test; #compared with the two independent samples t-test

TABLE 2. Pathological results of the 285 solitary pulmonary nodules (SPNs) included in this study

SPNs	Pathology	Datum (%)
Benign SPNs (n = 118)		
	Tuberculosis	46 (29.0%)
	Acute and chronic inflammation	32 (27.1%)
	Inflammatory pseudotumor	14 (11.9%)
	Hamartoma	9 (7.6%)
	Pulmonary sclerosing hemangioma	6 (5.1%)
	Sequestration	4 (3.4%)
	Bronchogenic cyst	3 (2.5%)
	Rheumatoid arthritis	2 (1.7%)
	Granulomatosis with polyangiitis	2 (1.7%)
Malignant SPNs (n = 167)		
	Primary pulmonary carcinoma	116 (69.5%)
	Solitary metastasis	23 (13.8%)
	Primary lung neuroendocrine tumor	21 (12.6%)
	Primary pulmonary lymphoma	7 (4.2%)

TABLE 3. Solitary pulmonary nodules evaluated with non-contrast enhanced CT

CT findings*	Benign SPNs (n = 118)	Malignant SPNs (n = 167)	*P* Values
Smooth margin			
Yes	84 (71.19%)	49 (29.34%)	< 0.0001
No	34 (28.81%)	118 (70.66%)	
Lobulated sign			
Yes	29 (24.58%)	115 (68.86%)	< 0.0001
No	89 (75.42%)	52 (31.14%)	
Spiculated sign			
Yes	25 (21.19%)	108 (78.81%)	< 0.0001
No	93 (64.67%)	59 (35.33%)	
Vacuole sign			
Yes	13 (11.02%)	38 (22.75%)	0.0120
No	105 (88.98%)	129 (77.25%)	
Cavity sign			
Yes	9 (7.63%)	16 (9.58%)	0.6727
No	109 (92.37%)	151 (90.42%)	
Air bronchogram			
Yes	33 (27.97%)	56 (33.53%)	0.3643
No	85 (72.03%)	111 (66.47%)	
Calcification			
Yes	10 (8.47%)	6 (3.59%)	0.1149
No	108 (91.53%)	161 (96.41%)	
Fat			
Yes	6 (5.08%)	4 (2.40%)	0.3277
No	112 (94.92%)	163 (97.60%)	
Pleural indentation			
Yes	25 (21.19%)	89 (53.29%)	< 0.0001
No	93 (78.81%)	78 (46.71%)	
Vessel convergence			
Yes	33 (27.97%)	84 (50.30%)	0.0002
No	85 (72.03%)	83 (49.70%)	
Adjacent bronchial changes			
Yes	26 (22.03%)	43 (25.75%)	0.4867
No	92 (77.97%)	124 (74.25%)	
Location			
Upper and middle lobes	53 (44.92%)	79 (47.31%)	0.7186
Inferior lobe	65 (55.08%)	88 (52.69%)	
Size (mm)			
15–20	29 (24.58%)	46 (27.54%)	0.5883
20–30	89 (75.42%)	121 (72.46%)	

SPNs = solitary pulmonary nodules; *compared with the Fisher's exact test

For the classification of SPNs (Table 4), among the 118 benign SPNs, there were 39, 9, 48, 22, and 0 SPNs that were classified as the Category I, II, III, IV, and V nodules, respectively. Among the 167 malignant SPNs, there were 0, 5, 54, 19, and 89 SPNs that were classified as the Category I, II, III, IV, and V nodules, respectively.

For CECT, among the 167 malignant SPNs, 118 cases (70.66%, 118/167) were noted with a CT enhancement amplitude value of 20–60 HU; and among the 118 benign SPNs, 75 cases (63.56%, 75/118) were noted with a CT enhancement amplitude value of less than 20 HU or more than 60 HU (Figure 3).

CTPI in evaluating SPNs

The parameters of BF, BV, MTT, and PS of CTPI in malignant SPNs were higher than those of benign SPNs (Figure 4, Table 5). However, there was only significant difference in the PS parameter ($p < 0.05$). A ROC curve analysis was performed on the PS parameter for differentiating benign and malignant SPNs (Figure 5). It showed an AUC of 0.739 (95% confidence interval of 0.684–0.789, $p < 0.0001$) with the sensitivity, specificity, and diagnostic threshold of 85.03 %, 66.10%, and 9.88 ml/100g/min, respectively.

DECT in evaluating SPNs

For DECT in evaluating SPNs (Figure 6), parameters of aOL, vOL, aIC, vIC, aNIC, and vNIC in malignant SPNs were significantly higher than those of benign SPNs (all p values were < 0.05, Table 6). ROC curve analyses were performed on these parameters for differentiating benign and malignant SPNs (Figure 7). The AUCs, sensitivities, and specificities were 0.636 to 0.790, 59.88% to 75.45%, and 61.02% to 80.51%, respectively. The diagnostic thresholds were 13.89 HU, 12.79 HU, 0.65 mg/ml, 0.85 mg/ml, 0.12, and 0.35, respectively (Table 7). Compared with the AUC of aOL, vOL, aIC, vIC, and aNIC by the Delong test, vNIC had the largest AUC (all p values < 0.05, Table 8).

Multimodality CT imaging in evaluating SPNs

For methods A, B, C, A+B, A+C, B+C, and A+B+C, the sensitivities, specificities, accuracies, PPVs, and NPVs were 83.23% to 97.60%, 63.56% to 88.14%, 75.09% to 93.68%, 76.37% to 92.09%, and 72.82% to 96.30%, respectively (Table 9).

There were no significant differences between the methods A, B, and C in sensitivities, specificities, and accuracies, and so did the methods A+B, A+C, B+C, and A+B+C (all p values > 0.05). However, the methods A+B, A+C, B+C, and A+B+C all had higher sensitivities, specificities, and accuracies than the methods A, B, and C for distinguishing benign from malignant SPNs (all p values < 0.05).

Discussion

NECT and CECT in evaluating SPNs

As low-dose CT scanning is more and more widely used in the early screening of lung cancers, to some extent, NECT scanning has become one of the most commonly used examination modalities for SPNs.[12] In addition to confirming the location, NECT is also used to perform a morphologic evaluation of SPNs. Generally speaking, the smaller the SPN, the more likely it is to be a benign lesion. In terms of the margins and contours of an SPN, it can be classified as smooth, lobulated, irregular, or spiculated.[1,5,6] Studies have reported that about 80% of benign SPNs are not larger than 2.0 cm in diameter.[1,5,6,13] However, some studies showed that about 15% of malignant SPNs are not larger than 1.0 cm in diameter, and 42% of malignant SPNs are not larger than 2.0 cm in diameter.[1,14] Most benign SPNs have smooth and well-defined margins. However, about 21% of malignant SPNs have well-defined margins.[15] A lobulated, irregular, or spiculated contour is usually associated with a malignant SPN. However, lobulation also occurs in up to 25% of benign SPNs.[16] Therefore, there are considerable overlaps in the size, margins, and contours of benign and malignant SPNs. Internal characteristics (*e.g.* homogeneous attenuation, cavitation, intranodular fat, presence and pattern of intranodular calcification, *etc.*) and abnormalities surrounding nodules (*e.g.* pleural indentation, vessel convergence, adjacent bronchial changes, *etc.*) are also helpful for distinguishing benign from malignant SPNs.[1] For example, intranodular fat and a popcorn like calcification are typical findings seen in hamartomas. However, intranodular fat or calcification alone cannot be used to differentiate benign from malignant SPNs confidently.

In our study, there were significant differences between the malignant and benign SPNs only in smooth margins (29.34% *vs* 71.19%), lobulated sign (68.86% *vs* 24.58%), spiculated sign (78.81% *vs* 21.19%), vacuole sign (22.75% *vs* 11.02%), pleural indentation (53.29% *vs* 21.19%), and vessel con-

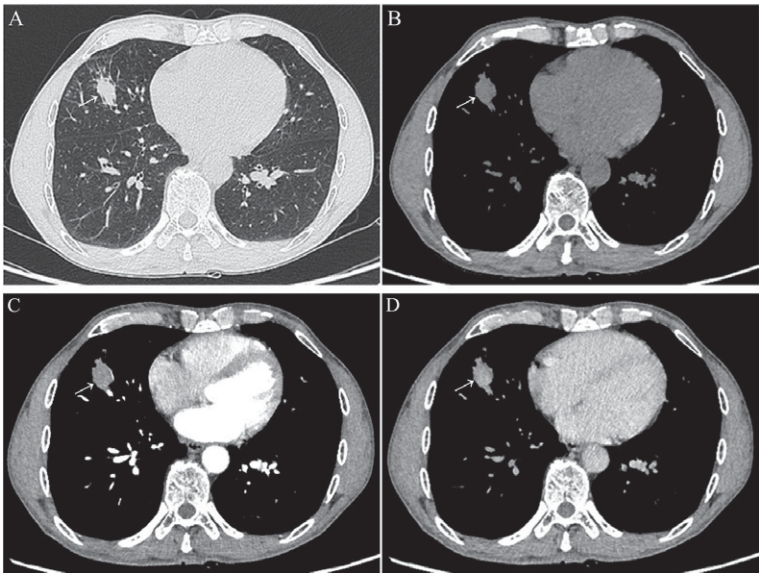

FIGURE 3. A solitary pulmonary nodule (SPN) with the size of 17.0 × 19.0 mm located in the middle lobe of right lung of a 59 years old male. Non-contrast enhanced CT (NECT), both upper **(A)** and **(B)** images, showed that there was sign of smooth margin, but without signs of lobulation, spiculation, vacuole, cavitation, air bronchogram, calcification, fat, pleural indentation, vessel convergence, or adjacent bronchial changes. Contrast enhanced CT (CECT) showed that there were mild and obvious enhancements in the arterial **(C)** and venous **(D)** phases, respectively. The patient was scanned with a CT-guided percutaneous lung biopsy procedure, and the pathological result showed chronic inflammatory disease. This SPN disappeared after a week of antibiotic therapy.

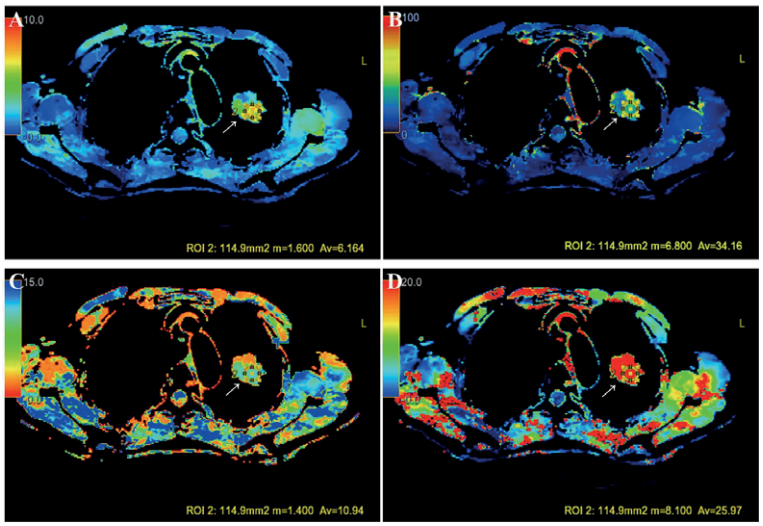

FIGURE 4. A solitary pulmonary nodule (SPN) with the size of 25.0 × 27.0 mm located in the superior lobe of left lung of a 61 years old female evaluated by CT perfusion imaging (CTPI). Blood volume (BV) **(A)**, blood flow (BF) **(B)**, mean transit time (MTT) **(C)**, and permeability surface (PS) **(D)** for the SPN were 6.16 ml/100 g, 34.16 ml/100 g/min, 10.94 s, and 25.97 ml/100 g/min, respectively. Pathology of the SPN after the surgery confirmed the diagnosis of an adenocarcinoma.

TABLE 4. Non-enhanced computed tomography (NECT) in evaluating solitary pulmonary nodules (SPNs) with various categories in 285 patients

Items	Category I	Category II	Category III	Category IV	Category V
Benign SPNs (n = 118)	39	9	48	22	0
Malignant SPNs (n = 167)	0	5	54	19	89

Category I = most likely benign; Category II = possibly benign; Category III = uncertain benign or malignant; Category IV = possibly malignant; Category IV = most likely malignant

TABLE 5. Solitary pulmonary nodules evaluated with CT perfusion imaging

Parameters*	Benign SPNs (n = 118)	Malignant SPNs (n = 167)	*P* values
BF (ml/100 g/min)	49.34 (27.78, 72.81)	58.44 (24.91, 80.47)	0.1022
BV (ml/100 g)	4.79 (2.87, 7.66)	4.84 (2.90, 7.74)	0.1829
MTT (s)	6.71 (3.05, 9.58)	7.66 (3.83, 10.54)	0.2034
PS (ml/100 g/min)	8.89 (4.94, 12.45)	14.37 (11.50, 16.29)	< 0.0001

BF = blood flow; BV = blood volume; CT = computed tomography; MTT = mean transit time; PS = permeability surface; SPNs = solitary pulmonary nodules; *compared with the Mann Whitney rank sum test

TABLE 6. Solitary pulmonary nodules (SPNs) evaluated with dual-energy CT

Parameters*	Benign SPNs (n = 118)	Malignant SPNs (n = 167)	*P* Values
aOL (HU)	13.24 (10.97, 21.58)	19.58 (13.29, 26.07)	< 0.0001
vOL (HU)	11.09 (10.09, 14.86)	14.99 (10.59, 23.98)	< 0.0001
aIC (mg/ml)	0.69 (0.47, 0.985)	1.13 (0.70, 1.56)	< 0.0001
vIC (mg/ml)	0.55 (0.44, 1.00)	0.97 (0.50, 1.46)	< 0.0001
aNIC	0.10 (0.06, 0.13)	0.18 (0.11, 0.25)	< 0.0001
vNIC	0.23 (0.13, 0.32)	0.54 (0.43, 0.65)	< 0.0001

aIC = Iodine concentration at the arterial phase; aNIC = normalized iodine concentration at the arterial phase; aOL = Iodine overlay at the arterial phase; CT = computed tomography; HU = Hounsfield unit; SPNs = solitary pulmonary nodules; vIC = Iodine concentration at the venous phase; vNIC = normalized iodine concentration at the venous phase; vOL = Iodine overlay at the venous phase; *compared with the Mann Whitney rank sum test

vergence (50.30% *vs* 27.97%) on NECT (all p values < 0.05). Our results are consistent with some previous studies.[17-19] Some previous studies also reported that these findings on NECT are risk factors for malignant SPNs. However, we did not identify cavity sign, air bronchogram, calcification, fat, adjacent bronchial changes, location, or size as risk factors for malignant SPNs (all p values > 0.05). This may be explained by the number of patients with SPNs included in our and previous studies which varied largely. Our results and previous studies also showed considerable overlaps in the findings of benign and malignant SPNs on NECT. Therefore, when we performed the classification of the 285 SPNs, there were 157 cases that were classified as the Category II, III, and IV nodules.

For CECT, it is helpful to improve the accuracy of differential diagnosis between benign and malignant SPNs. The degree of enhancement is directly associated with the possibility of malignancy and the vascularity of the SPNs. Swensen *et al.*[20] reported that nodular enhancement of more than 20 HU on CECT highly implies a malignant SPN. Whereas, nodular enhancement of less than 15 HU on CECT typically indicates a benign SPN, with a sensitivity, specificity, accuracy, PPV, and NPV of 98%, 58%, 77%, 68%, and 96%, respectively. In our study, the diagnostic criteria for CT enhancement were: a CT enhancement amplitude value of 20–60 HU was classified as malignant, and a CT enhancement amplitude value of less than 20 HU or more than 60 HU was classified as benign. We also want to highlight that CT postprocessing technology of thin-section and multiplanar reconstruction (MPR) are indeed beneficial when differentiating benign and malignant SPNs. This is because more details would be identified with thin-section CT and MPR. On the other hand, comprehensive morphological features evaluation is far better than a single morphological features assessment because more negative (or positive) morphological features will increase the likelihood of a malignant (or benign) SPN.

CTPI in evaluating SPNs

CTPI allows the derivation of several physiologic parameters, including BV, BF, MTT, and PS. BV is defined as the integral under a corrected attenuation curve for enhancement values from a contrast material bolus. It is a relative measure of the blood volume within small vessels in a region of specific tissue. BV is related to the number and diameter of open vessels, *etc.* MTT is a measure of the time it takes for blood to pass through small vessels. BF refers to the blood flow passing through a section of the blood vessel in unit time which is related

TABLE 7. Solitary pulmonary nodules evaluated with dual-energy CT

Parameters	AUC	Threshold	Sensitivity	Specificity	95% CI	*P* values
aOL (HU)	0.636	13.89	70.66	61.02	0.577–0.692	< 0.001
vOL (HU)	0.638	12.79	59.88	72.03	0.580–0.694	< 0.001
aIC (mg/ml)	0.657	0.65	67.66	69.49	0.599–0.712	< 0.001
vIC (mg/ml)	0.703	0.85	68.86	71.19	0.646–0.755	< 0.001
aNIC	0.728	0.12	67.66	74.58	0.672–0.778	< 0.001
vNIC	0.790	0.35	75.45	80.51	0.738–0.836	0.0001

aIC = Iodine concentration at the arterial phase; aNIC = normalized iodine concentration at the arterial phase; aOL = Iodine overlay at the arterial phase; AUC = area under the curve; CT = computed tomography; HU = Hounsfield unit; vIC = Iodine concentration at the venous phase; vOL = Iodine overlay at the venous phase; vNIC = normalized iodine concentration at the venous phase

95 % CI = 95 % confidence interval

TABLE 8. Pairwise comparison of AUC of dual energy CT parameters in 285 patients with solitary pulmonary nodules

Parameters*	*Z* statistic	*P* value
aOL *vs* vOL	0.0995	0.9207
aOL *vs* aIC	0.813	0.4162
aOL *vs* vIC	2.485	0.0129
aOL *vs* aNIC	3.171	0.0015
aOL *vs* vNIC	5.170	< 0.0001
vOL *vs* aIC	0.702	0.4829
vOL *vs* vIC	2.567	0.0103
vOL *vs* aNIC	3.280	0.0010
vOL *vs* vNIC	5.345	< 0.0001
aIC *vs* vIC	2.034	0.0420
aIC *vs* aNIC	2.755	0.0059
aIC *vs* vNIC	4.728	< 0.0001
vIC *vs* aNIC	1.036	0.3001
vIC *vs* vNIC	3.227	0.0013
aNIC *vs* vNIC	2.708	0.0068

aIC = Iodine concentration at the arterial phase; aOL = Iodine overlay at the arterial phase; aNIC = normalized iodine concentration at the arterial phase; AUC = area under the curve; CT = computed tomography; vIC = Iodine concentration at the venous phase; vNIC = normalized iodine concentration at the venous phase; vOL = Iodine overlay at the venous phase; *compared with the DeLong test

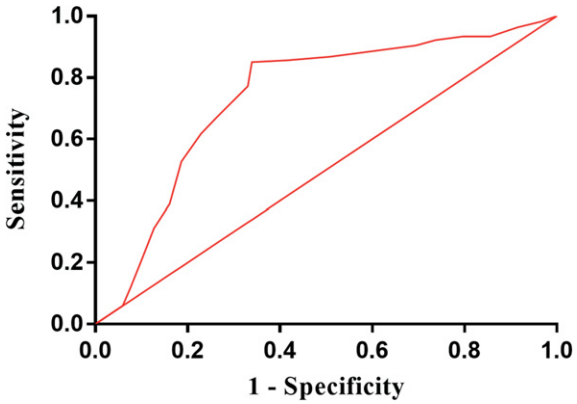

FIGURE 5. Receiver operating characteristic curve for distinguishing benign from malignant nodules using CT perfusion imaging parameter of permeability surface (PS).

to the patency of drainage vein, lymphatic reflux, blood volume level, *etc.* BF is calculated with the equation: BF = BV/MTT, where BV is blood volume and MTT is mean transit time. PS refers to the diffusion coefficient of the unidirectional transmission velocity of the contrast agent through capillary endothelial cells.

CTPI can be used to evaluate the perfusion and vascularity of lesions in the lung and many other organs.[21-28] Wang *et al.*[21] reported that parameters of CTPI (including BF, BV and PS but not MTT) of SPNs were significantly correlated with SPNs' microvessel density (MVD) and luminal vascular parameters such as luminal vascular number (LVN), luminal vascular area (LVA), and luminal vascular perimeter (LVP). Huang *et al.*[22] analyzed the CT perfusion parameters (BF, BV, MTT, and PS) and the microvessel parameters (MVD, LVN, LVA, and LVP) in the non-small cell lung cancer (NSCLC) patients with and without lymph node metastasis.

In our study, only the PS parameter of CTPI was found to be significant difference between the malignant and benign SPNs ($p < 0.05$), and a ROC curve analysis performed on the PS parameter showed that the AUC, sensitivity, specific-

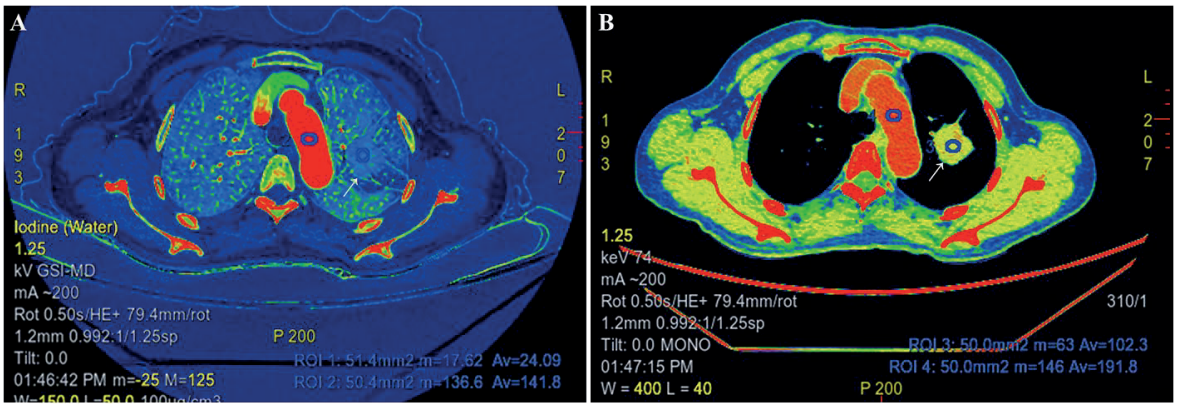

FIGURE 6. A solitary pulmonary nodule (SPN) with the size of 24.0 × 26.0 mm located in the superior lobe of left lung of a 57 years old female evaluated by arterial **(A)** and venous phases **(B)** of dual-energy CT (DECT). Iodine concentration at the arterial phase (aIC), Iodine concentration at the venous phase (vIC), normalized iodine concentration at the arterial phase (aNIC), and normalized iodine concentration at the venous phase (vNIC) were 2.409 mg/mL, 10.23 mg/mL, 0.17 (2.409/14.18), 0.53 (10.23/19.18) respectively. Pathology of the SPN after the surgery confirmed the diagnosis of an adenocarcinoma.

ity, and diagnostic threshold were 0.739, 85.03%, 66.10%, and 9.88 ml/100g/min, respectively. Our results are not completely consistent with previous reports.[7,8,29] For example, in the systematic review and meta-analysis performed by Huang *et al.*[8], lung cancer was found having higher BV, BF, MTT, and PS values than benign lesions; and AUC values of BV and PS were 0.92 (0.90, 0.94) and 0.83 (0.80, 0.86), respectively. The explanations may be as follow. PS mainly reflects the structural integrity of the capillary wall and the osmotic pressure between plasma and tissue fluid. There are a large number of microvessels and rich blood supply in malignant tumors. However, the capillary wall is immature, which is mainly reflected in the incomplete structure of vascular wall, including the basement membrane and epithelial cells. As a result, the vascular permeability will increase, promoting a large number of contrast agents to enter the tissue space. By contrast, the capillary wall of benign nodules is mature with a complete basement membrane and continuous endothelial cells which decreases the contrast agents to enter into the tissue space. On the other hand, although there are abundant microvessels in inflammatory lesions in benign nodules, in addition to the mature development of vascular wall, the edema and congestion of surrounding tissues will lead to the increase of tissue hydrostatic pressure which will also slow down the penetration rate of contrast medium. Therefore, the overall result is that the PS value in malignant SPNs was higher than that of benign SPNs.

TABLE 9. Solitary pulmonary nodules evaluated with multimodality CT imaging

Methods*	Sensitivity (%)	Specificity (%)	Accuracy (%)	PPV (%)	NPV (%)
Method A	83.23	63.56	75.09	76.37	72.82 %
Method B	85.63	67.80	78.25	79.01	76.92 %
Method C	84.43	66.10	76.84	77.90	75.00 %
Method A+B	94.61	74.58	86.32	84.04	90.72 %
Method A+C	92.81	77.97	86.67	85.64	88.46 %
Method B+C	95.81	81.36	89.82	87.91	93.20 %
Method A+B+C	97.60	88.14	93.68	92.09	96.30 %

CT = computed tomography; Method A = non-contrast enhanced CT combined with contrast enhanced CT; Method B = non-contrast enhanced CT combined with dual energy CT; Method C = non-contrast enhanced CT combined with CT perfusion imaging; Method A + B = non-contrast enhanced CT combined with contrast enhanced CT and dual energy CT; Method A + C = non-contrast enhanced CT combined with contrast enhanced CT and CT perfusion imaging; Method B + C = non-contrast enhanced CT combined with dual energy CT and CT perfusion imaging; Method A + B + C = non-contrast enhanced CT combined with contrast enhanced CT, dual-energy CT, and CT perfusion imaging; NPV = Negative predictive value; PPV = Positive predictive value; *compared with the McNemar's test

DECT in evaluating SPNs

There are mainly three techniques commercially available for DECT scanning. These techniques include: (a) fast voltage switching DECT, (b) layer detector DECT, and (c) dual-source DECT.[30] In this study, we used a fast voltage switching DECT system. It has the ability to obtain virtual nonenhanced images, arterial phase and venous phase contrast enhanced images, and iodine maps in one examination.[30]

An iodine map is the decomposition of material components realized by dual DECT according to the different attenuation characteristics of substances under high and low energy. It is the imaging of iodine material density extracted from enhanced iodine components. Iodine maps can effectively inhibit the background CT value and match with artificial color maps which can directly reflect the difference in iodine concentration in the lesion. The iodine concentration in the lesions can be measured quantitatively, and the lesions with slight enhancement can be displayed more sensitively. The CT value of the lesions measured on the iodine maps is the net enhancement value of the lesions. By measuring the enhancement value of lesions in iodine maps, we can evaluate the hemodynamic changes of tumors and the curative effects after tumor treatments.

In our results, parameters of DECT, which included aOL, vOL, aIC, vIC, aNIC, and vNIC, in malignant SPNs, were significantly higher than those of benign SPNs (all p values < 0.05). Compared with the AUC of aOL, vOL, aIC, vIC, and aNIC, the vNIC had the largest AUC (all p values < 0.05). Our results are consistent with many previous publications.[9,10,31-34] For example, Ha *et al.*[31] differentiated pulmonary metastasis from benign lung nodules in thyroid cancer patients by using DECT parameters finding that the DECT parameters (IC, NIC, NIC in using pulmonary artery, λ_{HU}, and Z-effective values) of the metastatic nodules were significantly higher than those of the benign nodules (all p values < 0.05).

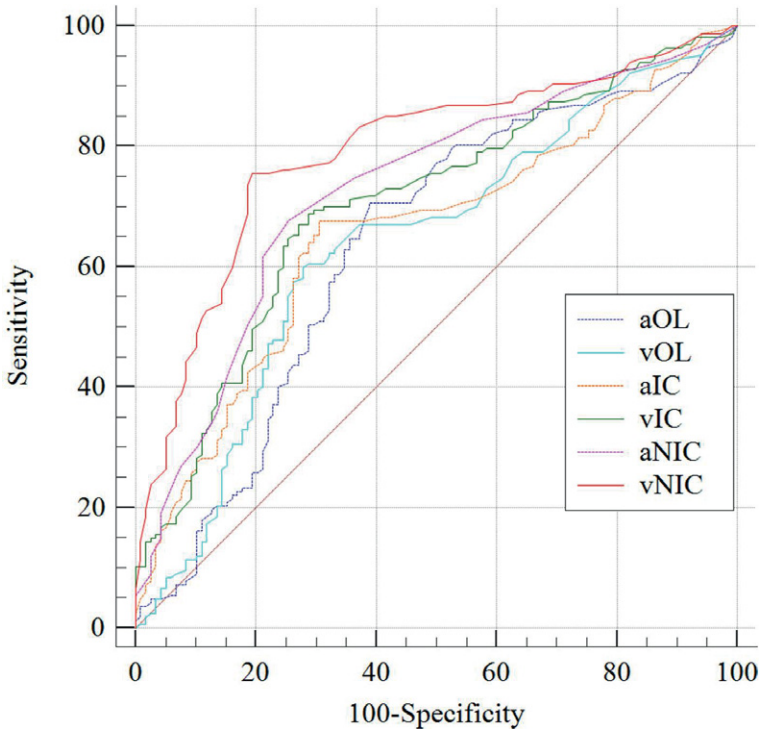

FIGURE 7. Receiver operating characteristic curves for distinguishing benign from malignant nodules using dual-energy CT parameters.

aOL = Iodine overlay at the arterial phase (AUC = 0.636); vOL = Iodine overlay at the venous phase (AUC = 0.638); aIC = Iodine concentration at the arterial phase (AUC = 0.657); vIC = Iodine concentration at the venous phase (area under the curve [AUC] = 0.703); aNIC = normalized iodine concentration at the arterial phase (AUC = 0.728); vNIC = normalized iodine concentration at the venous phase (AUC = 0.790); all p values < 0.05

Multimodality CT imaging in evaluating SPNs

Zhou *et al.*[35] analyzed the relationship between clinical data, tumor markers, chest high-resolution CT (HRCT), and pathology in patients with SPNs finding that a joint evaluation model had better diagnostic efficiency for the diagnosis of SPN with diameter ≤ 2.0 cm. In another study, Zhu *et al.*[9] reported that IC from DECT was significantly correlated with low-dose volume perfusion CT (VPCT) parameters (BF, BV, MTT, flow extraction product (FED), pulmonary nodule enhancement peak (PPnod), and VPCT parameters (BV, FED, and PPnod) had better diagnostic performance for SPN than DECT parameters (IC). Both of the above studies showed that multimodal evaluation is helpful in improving the diagnostic efficiency of SPNs.

In this study, the diagnostic performances of the three diagnostic methods were separately used or in combination for differentiating benign and malignant SPNs were calculated, and the results showed that multimodality CT imaging had higher performances than single modality CT imaging in differentiating between benign and malignant SPNs in sensitivity, specificity, and accuracy (all p values < 0.05). To the best of the authors' knowledge, this is the first study in the literature in which NECT, CECT, CTPI and DECT were comprehensibly used to differentiate benign from malignant SPNs.

TABLE 10. Step-wise approach of multimodality CT imaging for evaluating solitary pulmonary nodules[1,46,47]

Non-contrast enhanced CT	Density	1. Solid
		2. Subsolid
	Shape	3. Round or oval
		4. Triangular or polygonal
	Margins	5. Smooth
		6. Lobulated
		7. Spiculated
	Internal characteristics	8. Fat
		9. Calcification
		10. Cavitation
	Some complex findings	11. Pleural retraction
		12. Air bronchogram
		13. Bubble like lucencies (pseudocavitation)
		14. Cystic airspace
		15. Vascular convergence
Contrast enhanced CT	Parameter (s)	16. Degree of enhancement
CT perfusion imaging	Parameter (s)	17. Permeability surface
Dual-energy CT	Parameter (s)	18. Normalized iodine concentration at the venous phase

Radiation in multimodality CT imaging

Radiation is an important consideration when using a multimodality CT imaging protocol. Previous studies have reported that the radiation dose of CTPI is the key factor hindering its application.[9,36] In our study, the $CTDI_{vol}$, DLP, and ED in the SPNs were 66.88 ± 4.36 mGy, 768.29 ± 91.65 mGy.cm, and 10.76 ± 1.18 mSv, respectively. We have tried to make the radiation dose in our study at an acceptable level by using low tube voltage, SmartmA, and iterative reconstruction.[37-39] Tube voltage and tube current are positively correlated with the radiation dose.[40-42] In addition, it is recommended that postset ASIR-V% (60% in this study) should be higher than or equal to preset ASIR-V% (50% in this study).[43-45] All these radiation reduction techniques have been shown to decrease the radiation dose while maintaining the image quality.[40-45]

Some limitations of this study are: (a) only a fast voltage switching DECT was used in our study, and we did not compare our results with parameters from a layer detector DECT or dual-source DECT; (b) we did not compare our results with parameters from a magnetic resonance imaging (MRI) or positron emission tomography computed tomography (PET/CT); (c) some parameters of CTPI and DECT were not included into our study for evaluating; (d) radiation dose of our multimodality CT imaging protocol is still at a relatively high level; and (e) we did not include some advanced medical image analysis methods, such as artificial intelligence (AI), deep learning, or radiomics in our study. As a result, further investigations are needed to strengthen our findings in the future.

Conclusions

In conclusion, SPNs evaluated with multimodality CT imaging contributes to improving the diagnostic accuracy of benign and malignant SPNs (Table 10). NECT helps to locate and evaluate the morphological characteristics of SPNs. CECT helps to evaluate the vascularity of SPNs. CTPI using parameter of PS and DECT using parameter of vNIC both are helpful for improving the diagnostic performance.

Acknowledgments

The authors would like to thank co-authors AB and MM for their help in editing and proofreading the article. This study was supported by grants

from the Sichuan Provincial Commission of Health (Nos. 18PJ138, 19PJ283, 19PJ284, and 20PJ284), the Sichuan Provincial Department of Science and Technology (No. 2019YFQ0028), the Science and Technology Association of Suining City (Nos. 6 and 10), and the Science and Technology Bureau of Mianyang City (No. 2020YJKY004).

References

1. Erasmus JJ, Connolly JE, McAdams HP, Roggli VL. Solitary pulmonary nodules: Part I. Morphologic evaluation for differentiation of benign and malignant lesions. *Radiographics* 2000; **20:** 43-58. doi: 10.1148/radiographics.20.1.g00ja0343
2. Kastner J, Hossain R, Jeudy J, Dako F, Mehta V, Dalal S, et al. Lung-RADS Version 1.0 versus Lung-RADS Version 1.1: comparison of categories using nodules from the national lung screening trial. *Radiology* 2021; **300:** 199-206. doi: 10.1148/radiol.2021203704
3. Truong MT, Ko JP, Rossi SE, Rossi I, Viswanathan C, Bruzzi JF, et al. Update in the evaluation of the solitary pulmonary nodule. *Radiographics* 2014; **34:** 1658-79. doi: 10.1148/rg.346130092
4. Wyker A, Henderson WW. Solitary Pulmonary Nodule. 2021 Jul 26. In: StatPearls [Internet]. Treasure Island (FL): StatPearls Publishing; 2021. PMID: 32310603
5. MacMahon H, Naidich DP, Goo JM, Lee KS, Leung ANC, Mayo JR, et al. Guidelines for management of incidental pulmonary nodules detected on CT images: from the Fleischner Society 2017. *Radiology* 2017; **284:** 228-43. doi: 10.1148/radiol.2017161659
6. Bueno J, Landeras L, Chung JH. Updated Fleischner Society Guidelines for managing incidental pulmonary nodules: common questions and challenging scenarios. *Radiographics* 2018; **38:** 1337-50. doi: 10.1148/rg.2018180017
7. Sun Y, Yang M, Mao D, Lv F, Yin Y, Li M, et al. Low-dose volume perfusion computed tomography (VPCT) for diagnosis of solitary pulmonary nodules. *Eur J Radiol* 2016; **85:** 1208-18. doi: 10.1016/j.ejrad.2016.03.026
8. Huang C, Liang J, Lei X, Xu X, Xiao Z, Luo L. Diagnostic performance of perfusion computed tomography for differentiating lung cancer from benign lesions: a meta-analysis. *Med Sci Monit* 2019; **25:** 3485-94. doi: 10.12659/MSM.914206
9. Zhu B, Zheng S, Jiang T, Hu B. Evaluation of dual-energy and perfusion CT parameters for diagnosing solitary pulmonary nodules. *Thorac Cancer* 2021; **12:** 2691-7. doi: 10.1111/1759-7714.14105
10. Wen Q, Yue Y, Shang J, Lu X, Gao L, Hou Y. The application of dual-layer spectral detector computed tomography in solitary pulmonary nodule identification. *Quant Imaging Med Surg* 2021; **11:** 521-32. doi: 10.21037/qims-20-2
11. DeLong ER, DeLong DM, Clarke-Pearson DL. Comparing the areas under two or more correlated receiver operating characteristic curves: a nonparametric approach. *Biometrics* 1988; **44:** 837-45. PMID: 3203132
12. Lv E, Liu W, Wen P, Kang X. Classification of benign and malignant lung nodules based on deep convolutional network feature extraction. *J Healthc Eng* 2021; **2021:** 8769652. doi: 10.1155/2021/8769652
13. Borghesi A, Michelini S, Nocivelli G, Silva M, Scrimieri A, Pezzotti S, et al. Solid indeterminate pulmonary nodules less than or equal to 250 mm3: application of the updated Fleischner Society Guidelines in clinical practice. *Radiol Res Pract* 2019; **2019:** 7218258. doi: 10.1155/2019/7218258
14. Yang W, Sun Y, Fang W, Qian F, Ye J, Chen Q, et al. High-resolution computed tomography features distinguishing benign and malignant lesions manifesting as persistent solitary subsolid nodules. *Clin Lung Cancer* 2018; **19:** e75-83. doi: 10.1016/j.cllc.2017.05.023
15. Borghesi A, Michelini S, Scrimieri A, Golemi S, Maroldi R. Solid indeterminate pulmonary nodules of less than 300 mm3: application of different volume doubling time cut-offs in clinical practice. *Diagnostics* 2019; **9:** 62. doi: 10.3390/diagnostics9020062
16. McDonald JS, Koo CW, White D, Hartman TE, Bender CE, Sykes AG. Addition of the Fleischner Society Guidelines to chest CT examination interpretive reports improves adherence to recommended follow-up care for incidental pulmonary nodules. *Acad Radiol* 2017; **24:** 337-44. doi: 10.1016/j.acra.2016.08.026
17. Xu DM, van der Zaag-Loonen HJ, Oudkerk M, Wang Y, Vliegenthart R, Scholten ET, et al. Smooth or attached solid indeterminate nodules detected at baseline CT screening in the NELSON study: cancer risk during 1 year of follow-up. *Radiology* 2009; **250:** 264-72. doi: 10.1148/radiol.2493070847
18. Gould MK, Donington J, Lynch WR, Mazzone PJ, Midthun DE, Naidich DP, et al. Evaluation of individuals with pulmonary nodules: when is it lung cancer? Diagnosis and management of lung cancer, 3rd edition. American College of Chest Physicians evidence-based clinical practice guidelines. *Chest* 2013; **143(5 Suppl):** e93S-120S. doi: 10.1378/chest.12-2351
19. McWilliams A, Tammemagi MC, Mayo JR, Roberts H, Liu G, Soghrati K, et al. Probability of cancer in pulmonary nodules detected on first screening CT. *N Engl J Med* 2013; **369:** 910-9. doi: 10.1056/NEJMoa1214726
20. Swensen SJ, Viggiano RW, Midthun DE, Müller NL, Sherrick A, Yamashita K, et al. Lung nodule enhancement at CT: multicenter study. *Radiology* 2000; **214:** 73-80. doi: 10.1148/radiology.214.1.r00ja1473
21. Wang M, Li B, Sun H, Huang T, Zhang X, Jin K, et al. Correlation study between dual source CT perfusion imaging and the microvascular composition of solitary pulmonary nodules. *Lung Cancer* 2019; **130:** 115-20. doi: 10.1016/j.lungcan.2019.02.013
22. Huang T, Sun H, Luo X, Zhang X, Jin K, Wang F, et al. Correlation study between flash dual source CT perfusion imaging and regional lymph node metastasis of non-small cell lung cancer. *BMC Cancer* 2020; **20:** 547. doi: 10.1186/s12885-020-07032-8
23. Marin A, Murchison JT, Skwarski KM, Tavares AAS, Fletcher A, Wallace WA, et al. Can dynamic imaging, using 18F-FDG PET/CT and CT perfusion differentiate between benign and malignant pulmonary nodules? *Radiol Oncol* 2021; **55:** 259-67. doi: 10.2478/raon-2021-0024
24. Ostman C, Garcia-Esperon C, Lillicrap T, Tomari S, Holliday E, Levi C, et al. Multimodal computed tomography increases the detection of posterior fossa strokes compared to brain non-contrast computed tomography. *Front Neurol* 2020; **11:** 588064. doi: 10.3389/fneur.2020.588064
25. Li Q, Cui D, Feng Y, He Y, Shi Z, Yang R. Correlation between microvessel density (MVD) and multi-spiral CT (MSCT) perfusion parameters of esophageal cancer lesions and the diagnostic value of combined CtBP2 and $P16^{INK4A}$. *J Gastrointest Oncol* 2021; **12:** 981-90. doi: 10.21037/jgo-21-247
26. Zaboriene I, Zviniene K, Lukosevicius S, Ignatavicius P, Barauskas G. Dynamic perfusion computed tomography and apparent diffusion coefficient as potential markers for poorly differentiated pancreatic adenocarcinoma. *Dig Surg* 2021; **38:** 128-35. doi: 10.1159/000511973
27. Woolen S, Virkud A, Hadjiiski L, Cha K, Chan HP, Swiecicki P, et al. Prediction of disease free survival in laryngeal and hypopharyngeal cancers using CT perfusion and radiomic features: a pilot study. *Tomography* 2021; **7:** 10-19. doi: 10.3390/tomography7010002
28. Mathy RM, Fritz F, Mayer P, Klauss M, Grenacher L, Stiller W, et al. Iodine concentration and tissue attenuation in dual-energy contrast-enhanced CT as a potential quantitative parameter in early detection of local pancreatic carcinoma recurrence after surgical resection. *Eur J Radiol* 2021; **143:** 109944. doi: 10.1016/j.ejrad.2021.109944
29. Li Y, Yang ZG, Chen TW, JQ, Sun JY, Chen HJ, et. al. First-pass perfusion imaging of solitary pulmonary nodules with 64-detector row CT: comparison of perfusion parameters of malignant and benign lesions. *Brit J Radiol* 2010; **83:** 785-90. doi: 10.1259/bjr/58020866
30. Marin D, Boll DT, Mileto A, Nelson RC. State of the art: dual-energy CT of the abdomen. *Radiology* 2014; **271:** 327-42. doi: 10.1148/radiol.14131480
31. Ha T, Kim W, Cha J, Lee YH, Seo HS, Park SY, et al. Differentiating pulmonary metastasis from benign lung nodules in thyroid cancer patients using dual-energy CT parameters. *Eur Radiol* 2022; **32:** 1902-11. doi: 10.1007/s00330-021-08278-x
32. Zegadło A, Żabicka M, Kania-Pudło M, Maliborski A, Różyk A, Sośnicki W. Assessment of solitary pulmonary nodules based on virtual monochrome images and iodine-dependent images using a single-source dual-energy CT with fast kVp switching. *J Clin Med* 2020; **9:** 2514. doi: 10.3390/jcm9082514

33. Zhang Y, Cheng J, Hua X, Yu M, Xu C, Zhang F, et al. Can spectral CT imaging improve the differentiation between malignant and benign solitary pulmonary nodules? *PLoS One* 2016; **11:** e0147537. doi: 10.1371/journal.pone.0147537

34. Lin JZ, Zhang L, Zhang CY, Yang L, Lou HN, Wang ZG. Application of gemstone spectral computed tomography imaging in the characterization of solitary pulmonary nodules: preliminary result. *J Comput Assist Tomogr* 2016; **40:** 907-11. doi: 10.1097/RCT.0000000000000469

35. Zhou S, Wang Q, Tang T, Cao M, Tan Y, Bai K, et al. Joint prediction of solitary pulmonary module malignant probability based on logistic regression and malignant tendency comprehensive score. *J BUON* 2021; **26:** 1815-23. PMID: 34761588

36. Chae EJ, Song JW, Krauss B, Song KS, Lee CW, Lee HJ, et al. Dual-energy computed tomography characterization of solitary pulmonary nodules. *J Thorac Imaging* 2010; **25:** 301-10. doi: 10.1097/RTI.0b013e3181e16232

37. U.S. Food and Drug Administration. What are the radiation risks from CT? In: *Medical X-ray imaging*. Available at: https://www.fda.gov/radiation-emitting-products/medical-x-ray-imaging/what-are-radiation-risks-ct

38. McCollough CH, Bushberg JT, Fletcher JG, Eckel LJ. Answers to common questions about the use and safety of CT scans. *Mayo Clin Proc* 2015; **90:** 1380-92. doi: 10.1016/j.mayocp.2015.07.011

39. Yan G, Li H, Bhetuwal A, McClure MA, Li Y, Yang G, et al. Pleural effusion volume in patients with acute pancreatitis: a retrospective study from three acute pancreatitis centers. *Ann Med* 2021; **53:** 2003-18. doi: 10.1080/07853890.2021.1998594

40. Chen CW, Chen PA, Chou CC, Fu JH, Wang PC, Hsu SH, et al. Combination of adaptive statistical iterative reconstruction-V and lower tube voltage during craniocervical computed tomographic angiography yields better image quality with a reduced radiation dose. *Acad Radiol* 2019; **26:** e233-e40. doi: 10.1016/j.acra.2018.07.019

41. Ye K, Chen M, Li J, Zhu Q, Lu Y, Yuan H. Ultra-low-dose CT reconstructed with ASiR-V using SmartmA for pulmonary nodule detection and Lung-RADS classifications compared with low-dose CT. *Clin Radiol* 2021; **76:** 156.e1-156.e8. doi: 10.1016/j.crad.2020.10.014

42. Ren Z, Zhang X, Hu Z, Li D, Liu Z, Wei D, et al. Application of adaptive statistical iterative reconstruction-V with combination of 80 kV for reducing radiation dose and improving image quality in renal computed tomography angiography for slim patients. *Acad Radiol* 2019; **26:** e324-e32. doi: 10.1016/j.acra.2018.12.021

43. Tang H, Yu N, Jia Y, Yu Y, Duan H, Han D, et al. Assessment of noise reduction potential and image quality improvement of a new generation adaptive statistical iterative reconstruction (ASIR-V) in chest CT. *Br J Radiol* 2018; **91:** 20170521. doi: 10.1259/bjr.20170521

44. Afadzi M, Lysvik EK, Andersen HK, Martinsen ACT. Ultra-low dose chest computed tomography: effect of iterative reconstruction levels on image quality. *Eur J Radiol* 2019; **114:** 62-8. doi: 10.1016/j.ejrad.2019.02.021

45. Zhu Z, Zhao Y, Zhao X, Wang X, Yu W, Hu M, et al. Impact of preset and postset adaptive statistical iterative reconstruction-V on image quality in nonenhanced abdominal-pelvic CT on wide-detector revolution CT. *Quant Imaging Med Surg* 2021; **11:** 264-75. doi: 10.21037/qims-19-945

46. Snoeckx A, Reyntiens P, Desbuquoit D, Spinhoven MJ, Van Schil PE, van Meerbeeck JP, et al. Evaluation of the solitary pulmonary nodule: size matters, but do not ignore the power of morphology. *Insights Imaging* 2018; **9:** 73-86. doi: 10.1007/s13244-017-0581-2

47. Hansell DM, Bankier AA, MacMahon H, McLoud TC, Müller NL, Remy J. Fleischner Society: glossary of terms for thoracic imaging. *Radiology* 2008; **246:** 697-722. doi: 10.1148/radiol.2462070712